Energy 36 (2011) 1319–1323

Contents lists available at ScienceDirect

Energy

journal homepage: www.elsevier.com/locate/energy

Estimation of monthly solar radiation distribution for solar energy system analysis

C. Coskun [a,*], Z. Oktay [a], I. Dincer [b]

[a] Mechanical Engineering Department, Faculty of Engineering, Balikesir University, 10110 Balikesir, Turkey
[b] Faculty of Engineering and Applied Science, University of Ontario Institute of Technology (UOIT), 2000 Simcoe St. N., Oshawa, ON L1H 7K4, Canada

ARTICLE INFO

Article history:
Received 6 June 2010
Received in revised form
8 November 2010
Accepted 9 November 2010
Available online 22 December 2010

Keywords:
Probability density frequency
Global solar radiation
Solar energy
Energy
Exergy
Efficiency

ABSTRACT

The concept of probability density frequency, which is successfully used for analyses of wind speed and outdoor temperature distributions, is now modified and proposed for estimating solar radiation distributions for design and analysis of solar energy systems. In this study, global solar radiation distribution is comprehensively analyzed for photovoltaic (PV) panel and thermal collector systems. In this regard, a case study is conducted with actual global solar irradiation data of the last 15 years recorded by the Turkish State Meteorological Service. It is found that intensity of global solar irradiance greatly affects energy and exergy efficiencies and hence the performance of collectors.

1. Introduction

Solar energy has gained much attention from many industries and application areas in recent years [1,2]. Researchers mainly focus on five key research areas, which can be expressed as follows; a) improving efficiencies of solar thermal collector or PV/T systems [3], b) solar-based electricity generation by utilizing single or hybrid energy systems [4–8], c) solar-powered hydrogen generation [8,9], d) solar energy utilization in zero energy or sustainable energy buildings [10,11], e) feasibility of solar energy utilization for many industrial applications like solar drying process [12–14]. Knowledge of global solar radiation distribution is needed for design and analysis of solar energy systems. Many parameters affect the energy, exergy and conversion efficiencies and working conditions of collectors. One of the most important parameters is the intensity of solar irradiance. It directly affects the thermal collector efficiency and the intensity of the solar irradiance. Average solar radiation and system efficiency are used in general calculations. However, it is clear that accurate results cannot be predicted by this method. Monthly distribution of global solar radiation should be predicted for accurate solar energy calculations. The concept of probability density frequency is successfully applied in the analyses of wind speed [15,16] and outdoor temperature distribution [17] in literature. Many distribution methods such as Weibull and Rayleigh are successfully used in wind speed and wind energy analyses. In open literature, there is no such a study showing global solar radiation distribution as a parameter of the solar irradiance intensity. This study presents a new method to use this knowledge in solar energy calculations. In this regard, a case study is conducted with the past actual data for 15 years as recorded by the Turkish State Meteorological Service. As an application, the global solar radiation distribution of a the Turkish city is comprehensively analyzed.

2. Description of the method

This study presents a new solar energy distribution calculation approach to accurately determine the amount of converted useful solar energy. A new program is written, and input solar radiation data are then loaded into program using a text file. A sample of utilized global solar irradiation data for the month of June is shown in Fig. 1. After submitting solar radiation data, program arranges data according to solar radiation and hours as shown in Fig. 2. Subsequently, a time elapsed for the intensity of solar irradiation of 50 W interval is determined. The program performs probability calculations with respect to time elapsed for each solar radiation intensity as shown in Fig. 2. Here, the first column in the vertical plane shows the intensity of solar radiation at an interval of 50 W. The first line in the horizontal plane corresponds to the time of day.

* Corresponding author. Tel.: +90 266 612 1194/433; fax: +90 266 612 1257.
E-mail addresses: canco82@yahoo.com (C. Coskun), zuhal.oktay@gmail.com (Z. Oktay), ibrahim.dincer@uoit.ca (I. Dincer).

0360-5442/$ – see front matter © 2010 Elsevier Ltd. All rights reserved.
doi:10.1016/j.energy.2010.11.009

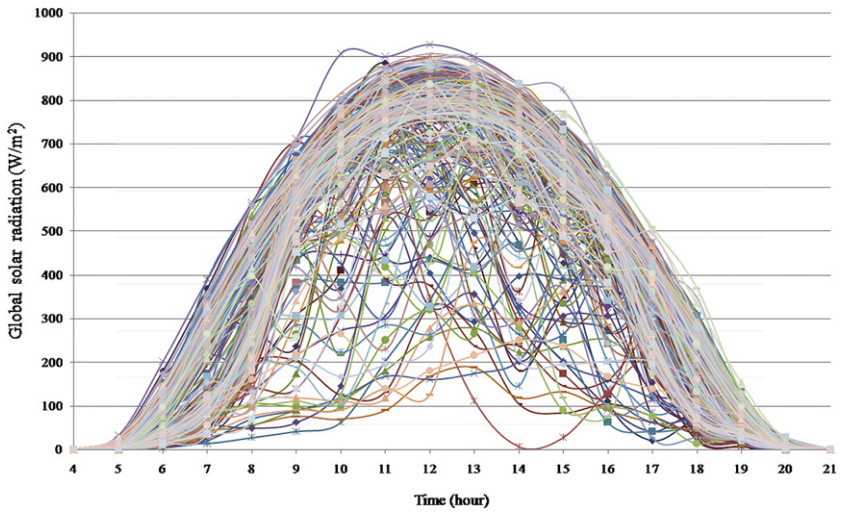

Fig. 1. Distribution of global solar irradiation for June.

Monthly-based total falling solar energy amount can be determined for 50 W intervals. For instance, 2.66 kW h/m^2 of solar radiation falls in the range of 600–650 W/m^2 and between 09:00 and 10:00 o'clock. Also, total solar energy amount can be indicated for 50 W intervals in the penultimate column. The last column in the vertical plane shows the total solar energy amount depending on the time of day. The last column shows the elapsed time.

A similar calculation is performed by Coskun [17] to estimate outdoor temperature distribution. He has proposed the sinusoidal function to estimate the probability density distribution of outdoor

Solar Radiation (W/m²)	Time: 5:00-6:00	6:00-7:00	7:00-8:00	8:00-9:00	9:00-10:00	10:00-11:00	11:00-12:00	12:00-13:00	13:00-14:00	14:00-15:00	15:00-16:00	16:00-17:00	17:00-18:00	18:00-19:00	Total Energy (kWh/m²)	Time lapsed (hour)
	Solar Energy (kWh/m²)															
0-50	0,42	0,06	0,008	-	-	-	-	-	-	-	-	0,015	0,081	0,495	1,079	43,16
50-100	0,546	0,724	0,062	0,055	0,032	0,009	-	-	-	0,03	0,052	0,057	0,488	0,894	2,949	39,32
100-150	0,826	0,571	0,134	0,051	0,096	0,053	0,012	0,011	0,05	0,04	0,085	0,103	0,583	0,326	2,941	23,53
150-200	0,115	0,172	0,499	0,036	0,017	0,055	0,051	0,036	0,018	0,037	0,037	0,276	0,682	0,048	2,079	11,88
200-250	0,04	0,856	1,267	0,151	0,044	0,043	0,024	0,045	0,132	0,112	0,089	0,714	1,333	-	4,85	21,56
250-300	-	1,53	1,155	0,141	0,054	0,11	0,107	0,136	0,195	0,195	0,161	1,103	1,555	-	6,442	23,43
300-350	-	1,098	0,622	0,126	0,186	0,64	0,232	0,13	0,163	0,166	0,232	1,384	0,227	-	5,206	16,02
350-400	-	0,226	0,865	0,185	0,111	0,117	0,038	0,073	0,076	0,23	0,644	1,892	0,132	-	4,589	12,24
400-450	-	-	1,758	0,35	0,128	0,218	0,213	0,292	0,086	0,26	0,856	3,483	-	-	7,644	17,99
450-500	-	-	1,859	1,189	0,341	0,14	0,241	0,143	0,186	1,045	1,473	0,701	-	-	7,318	15,41
500-550	-	-	1,132	2,798	0,784	0,373	0,267	0,322	0,472	1,09	4,647	0,153	-	-	12,038	22,93
550-600	-	-	0,392	5,262	0,932	0,345	0,694	0,675	1,155	2,083	5,101	-	-	-	16,639	28,94
600-650	-	-	-	3,681	2,66	0,945	0,756	0,957	1,567	3,59	1,173	-	-	-	15,329	24,53
650-700	-	-	-	1,736	5,152	1,694	1,626	1,699	2,86	5,15	0,066	-	-	-	19,983	29,60
700-750	-	-	-	0,283	5,133	4,245	1,739	2,259	4,213	3,535	-	-	-	-	21,407	29,53
750-800	-	-	-	-	2,845	6,273	6,065	5,96	6,115	0,23	-	-	-	-	27,488	35,47
800-850	-	-	-	-	0,488	4,83	5,495	5,584	2,858	0,082	-	-	-	-	19,337	23,44
850-900	-	-	-	-	0,09	1,903	4,453	3,379	-	-	-	-	-	-	9,825	11,23
	1,947	5,237	9,753	16,044	19,093	21,993	22,013	21,701	20,146	17,875	14,616	9,881	5,081	1,763	**187,14**	

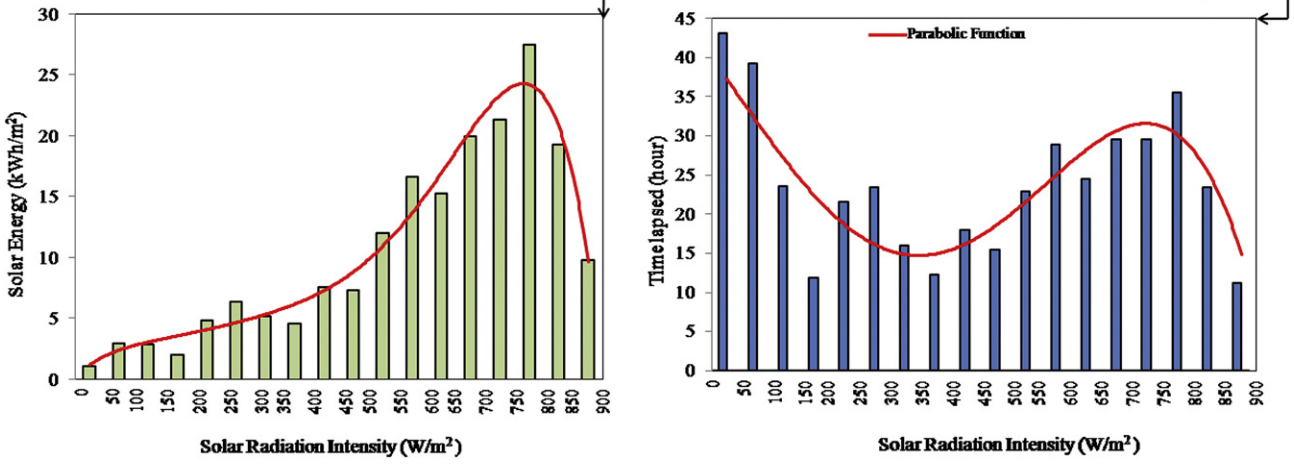

Fig. 2. Calculation results by the present method with respect to solar radiation intensity.

Table 1
Model parameters for each month considered.

Month	$H_x = a + b\cdot x + c\cdot x^2 + d\cdot x^3 + e\cdot x^4$					Global solar radiation (kW/m^2)	R^2
	a	b	c	d	e	$0 \le I \le s$	
January	122	−1306	6303	−13,021	9376	$0.00 \le I \le 0.55$	0.997
February	103	−920	3552	−5721	3180	$0.00 \le I \le 0.65$	0.991
March	80	−527	1545	−1792	658	$0.00 \le I \le 0.80$	0.989
April	95	−696	2088	−2472	978	$0.00 \le I \le 0.90$	0.974
May	61	−305	582	−180	−184	$0.00 \le I \le 0.90$	0.984
June	40	−104	−125	865	−713	$0.00 \le I \le 0.90$	0.917
July	36	−33	−493	1601	−1185	$0.00 \le I \le 0.90$	0.892
August	69	−502	1424	−1308	265	$0.00 \le I \le 0.85$	0.915
September	39	−139	71	787	−933	$0.00 \le I \le 0.80$	0.950
October	66	−440	1281	−1082	−93	$0.00 \le I \le 0.70$	0.984
November	86	−740	3009	−4874	2392	$0.00 \le I \le 0.55$	0.998
December	148	−1723	8786	−19,559	15,453	$0.00 \le I \le 0.45$	0.998

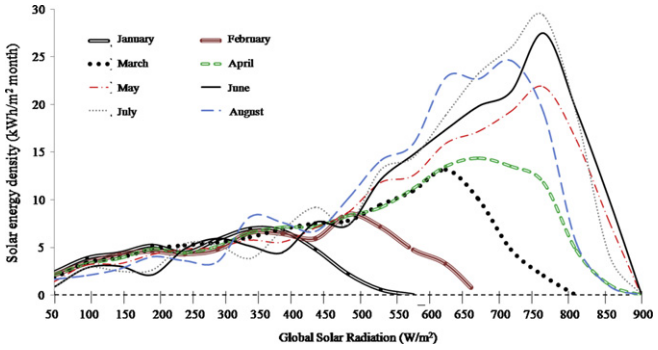

Fig. 3. Solar energy density distribution with global solar radiation intensity.

temperature. The present sinusoidal function is given in the following equation:

$$H(T_{out}) = a + b\cdot cos(c\cdot T_{out} + d) \quad (1)$$

where a, b, c and d are model parameters. T_{out} denotes outdoor temperature in °C. $H(T_{out})$ gives the hours elapsed in a month for T_{out}. In this analysis, the global solar radiation distribution is determined by using fourth degree parabola. It is found to have a better performance as

$$H(x) = a + b\cdot x + c\cdot x^2 + d\cdot x^3 + e\cdot x^4 \quad (2)$$

where a, b, c, d and e are model parameters. x denotes average intensity of global solar irradiance for 50 W solar radiation intervals in kW/m^2. $H(x)$ gives the time elapsed for 50 W solar radiation intervals. For instance, time elapsed between 100 and 150 W was found by using the average value of 0.125 kW in Eq. (1). After estimating the intensity of the global solar irradiance distribution, energy amount ($E(x)$) can be easily calculated for any range chosen for global solar irradiance as

$$E(x) = H(x)\cdot x = a\cdot x + b\cdot x^2 + c\cdot x^3 + d\cdot x^4 + e\cdot x^5 \quad (3)$$

$$E_{Total} = \sum_{n=0}^{k} E(n) \quad (4)$$

where 'k' indicates the global solar radiation limit for a given month. It is determined for the maximum solar radiation for each month depending on the actual solar data.

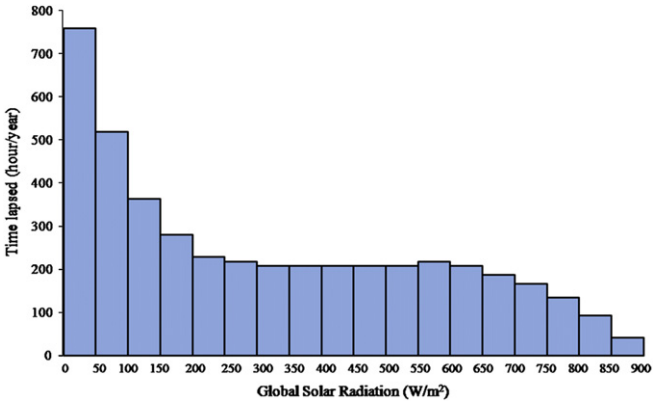

Fig. 5. Change in annual time lapse with intensity of the solar irradiance.

3. Results and discussion

Model parameters (a through e) and global solar radiation limits are calculated and given in Table 1 for Balikesir in Turkey. Time probability and solar energy distribution are calculated using Eqs. (1) and (2) for 12 months. To compare solar energy density distribution for each month, changes in solar energy density with increasing intensity of global solar radiation are shown in Fig. 3 for the first six months. The general trend shows that solar energy increases in parallel with the intensity of global solar radiation until it reaches the maximum and then begins to decline. The highest point reached in solar energy density changes among months in question. Changes in time probability frequency with the intensity of global solar radiation are shown in Fig. 4 for the first six months. As can be seen in Fig. 4, each distribution trend is different. Changes

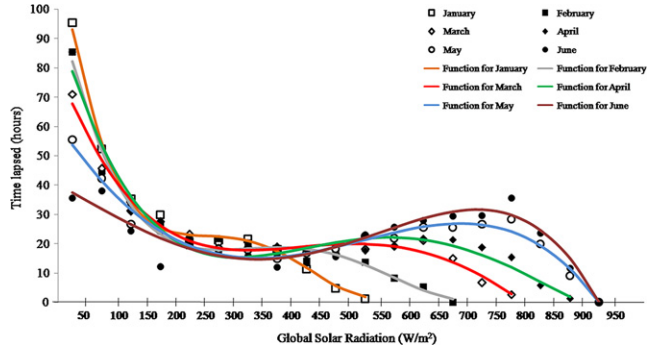

Fig. 4. Time probability intensity function for the first six months.

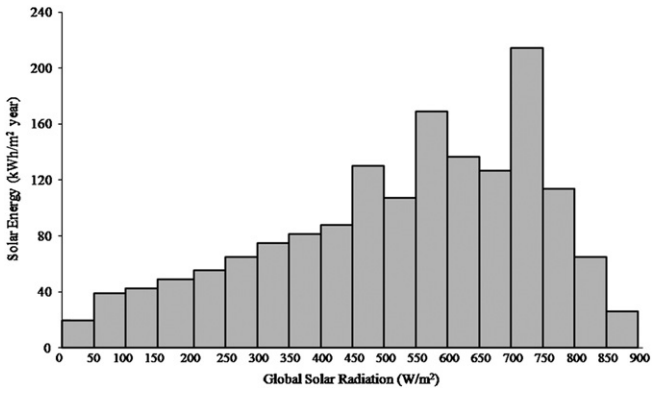

Fig. 6. Change in total solar energy with intensity of the solar irradiance.

Table 2
Thermal energy comparison for flat-plate type thermal collector.

Months	Average ambient temperature (°C)	Average solar radiation (W/m^2)	$T_{in} + T_{out}$ (°C)	Thermal energy for average values (kW h/m^2 month)	Thermal energy for new approach (kW h/m^2 month)
January	4.7	160	55	–	7.55
February	5.3	237	55	–	14.46
March	7.9	355	55	22.07	36.79
April	12.9	458	55	71.29	62.49
May	17.5	618	55	114.48	106.52
June	22.3	688	60	119.62	117.06
July	24.1	689	60	130.04	127.17
August	23.9	602	60	112.66	103.68
September	20.4	472	55	95.52	95.66
October	15.5	324	55	50.68	49.04
November	9.9	194	55	6.16	18.19
December	6.3	135	55	–	4.71

of annual time lapse and solar energy with the intensity of solar irradiance are investigated and shown in Figs. 5 and 6. There is no a clear relationship between the distribution of annual time lapse and solar energy with the intensity of solar irradiance. These two distributions have different trends.

In order to illustrate the present method and highlight its importance calculations are done for a case study. For this purpose, a sample analysis is conducted for both flat-plate type thermal collector and PV system. Energy efficiency function of flat-plate type thermal collector is taken from Ref. [18] as

$$\eta_{TC} = 0.74969 - 9.8748 \cdot m \tag{5}$$

$$m = \frac{((T_{in} + T_{out})/2) - T_{amb}}{x} \quad \left(^{\circ}\mathrm{C\,m^2/W}\right) \tag{6}$$

where T_{in} and T_{out} are the inlet and outlet temperatures of the fluid, while T_{amb} is the ambient temperature and x is the global solar radiation amount falling per m^2 (W/m^2). η_{TC} is the thermal collector energy efficiency. Peak power point function for the chosen photovoltaic system [19] per m^2 PV panel is given by

$$\mathrm{Pp}(x) = -12.378 + 0.382 \cdot x \cdot 2.73^{-0.003 \cdot T_{amb}} \tag{7}$$

where ambient temperature (T_{amb}) should be taken as Kelvin. Pp(x) is the peak power point (W/m^2). Energy efficiency of PV panel (η_{TC}) is described as

$$\eta_{PV} = \frac{\mathrm{Pp}(x)}{x} = \frac{-12.378 + 0.382 \cdot x \cdot 2.73^{-0.003 \cdot T_{amb}}}{x} \tag{8}$$

In Tables 2 and 3, the present model and a conventional calculation method are compared for each month. Differences between the present model and a conventional calculation method are found as 5.0% for PV system electricity generation.

Table 3
Electricity generation comparison for flat-plate type thermal collector.

Months	Electricity generation based on average values (kW h/m^2 month)	Electricity generation based on new approach (kW h/m^2 month)	Error (%)
January	4.10	4.91	16.49
February	6.15	6.77	9.15
March	11.67	12.22	4.50
April	14.95	15.52	3.67
May	21.78	22.28	2.24
June	25.22	25.93	2.73
July	26.05	26.48	1.62
August	21.02	21.66	2.95
September	16.88	17.30	2.42
October	10.60	11.05	4.07
November	5.69	6.91	17.65
December	2.39	3.32	28.01
Total	166.50	174.35	5.08

4. Conclusions

This paper has proposed the probability intensity function as a new method for estimating the solar irradiation. In the model, solar probability distribution and frequency are formulated as key parameters of the intensity of global solar irradiance. Some main findings of this study are given as follows:

- Time probability intensity frequency and probability power distribution with solar radiation intensity do not follow similar distribution patterns for each month.
- There is no relationship between the distribution of annual time lapse and solar energy with solar radiation intensity.
- The highest solar irradiation throughout the year remains between 700 and 750 W. This amount is equal to 213 kW h/year, which is 13.4% of the total annual solar irradiation reaching on a particular surface.
- Differences between the proposed model and conventional calculation method are found to be about 5.0% for a case study of PV-based electricity generation.
- The changes of annual time lapse become 200–230 h with solar radiation intensity between 200 and 700 W.

The present method is expected to be a potential tool for analysis and design of solar energy systems. It also helps develop solar radiation intensity maps for cities and countries.

Nomenclature

E	Energy (kW h)
H	Time elapsed in a month (h)
Pp	Peak power point (W/m^2)
T	Temperature (°C or K)
x	Global solar radiation (W/m^2 or kW/m^2)

Greek letters

η	Energy efficiency (−)

Subscripts

amb	Ambient
in	Inlet
out	Outlet
PV	Photovoltaic panel
TC	Thermal collector

References

[1] Wang RZ, Zhai XQ. Development of solar thermal technologies in China. Energy 2010;35(11):4407–16.
[2] Badescu V. Optimum size and structure for solar energy collection systems. Energy 2006;31:1819–35.
[3] Atkins MJ, Walmsley MRW, Morrison AS. Integration of solar thermal for improved energy efficiency in low-temperature-pinch industrial processes. Energy 2010;35:1867–73.
[4] Erdil E, Ilkan M, Egelioglu F. An experimental study on energy generation with a photovoltaic (PV)–solar thermal hybrid system. Energy 2008;33:1241–5.
[5] Reichling JP, Kulacki FA. Utility scale hybrid wind–solar thermal electrical generation: a case study for Minnesota. Energy 2008;33:626–38.
[6] Gou C, Ruixian C, Hui H. A novel hybrid oxy-fuel power cycle utilizing solar thermal energy. Energy 2007;32:1707–14.
[7] Rehman S, Luai MAH. Study of a solar PV–diesel–battery hybrid power system for a remotely located population near Rafha, Saudi Arabia. Energy 2010;35(12):4986–95.
[8] Guo LJ, Zhao L, Jing DW, Lu YJ, Yang HH, Bai BF, et al. Solar hydrogen production and its development in China. Energy 2009;34:1073–90.
[9] Liu Q, Jin H, Hong H, Sui J, Ji J, Dang J. Performance analysis of a mid- and low-temperature solar receiver/reactor for hydrogen production with methanol steam reforming. International Journal of Energy Research 2010; doi:10.1002/er.1738.
[10] Kalogirou SA, Bojic M. Artificial neural networks for the prediction of the energy consumption of a passive solar building. Energy 2000;25:479–91.
[11] Tiris C, Tiris M, Dincer I. Energy efficiency of a solar drying system. International Journal of Energy Research 1996;20(9):767–70.
[12] Midilli A, Kucuk H. Energy and exergy analyses of solar drying process of pistachio. Energy 2003;28:539–56.
[13] Dincer I. Evaluation and selection of energy storage systems for solar thermal applications. International Journal of Energy Research 1999;23(12):1017–28.
[14] Dincer I, Dost S. A perspective on thermal energy storage systems for solar energy applications. International Journal of Energy Research 1996;20(6):547–57.
[15] Celik AN. On the distributional parameters used in assessment of the suitability of wind speed probability density functions. Energy Conversion and Management 2004;45:1735–47.
[16] Carta JA, Ramírez P, Velázquez S. Influence of the level of fit of a density probability function to wind-speed data on the WECS mean power output estimation. Energy Conversion and Management 2008;49:2647–55.
[17] Coskun C. A novel approach to degree-hour calculation: indoor and outdoor reference temperature based degree-hour calculation. Energy 2010;35:2455–60.
[18] Gunerhan H, Hepbasli A. Exergetic modeling and performance evaluation of solar water heating systems for building applications. Energy and Buildings 2007;39:509–51.
[19] Akyuz E, Coskun C, Oktay Z, Dincer I. A novel approach for estimation of PV exergy efficiency. 2nd International Conference on Nuclear and Renewable Energy Resources (NURER), Ankara, Turkey; 2010.